An Experimental Study on Compression and Shrinkage Behavior of Cement Treated Marine Deposited Clays

By Abdullah Ekinci[1], Ceren Ince[2], Pedro Miguel Vaz Ferreira[3]

[1]Assistant Professor, European University of Lefke, Faculty of Engineering, Department of Civil Engineering, Lefke, Northern Cyprus, TR-10 Mersin, Turkey, Telephone: +90 (0) 5428881440, E-mail: aekinci@eul.edu.tr, https://orcid.org/0000-0002-6787-9983

[2]Assistant Professor, Civil Engineering Program, Middle East Technical University, Northern Cyprus Campus, Kalkanli, Guzelyurt, North Cyprus, via Mersin 10, Turkey, https://orcid.org/0000-0002-5210-0228

[3]Associate Professor, University College London, Gower Street, WC1E 6BT, London/UK, https://orcid.org/0000-0002-4626-7443

Abstract:

Marine clay deposits are commonly found soils around the world. Owing to the high costs of material disposal and the associated environmental problems, there is a growing need to find an alternative solution to reusing unsuitable soils. In the current study, the shrinkage and compression behavior of marine deposited clays, a soil commonly found worldwide, has been studied using intact, reconstituted, and cement treated samples. Additionally, the effect of cement inclusion was evaluated for dosages ranging from 1% to 7%. Furthermore, scanning electron microscopy (SEM) analysis and X-ray diffractometry were conducted to study the microstructural developments of cement treated clays. The results reported in this paper have important practical implications as they provide significant knowledge on the compressibility behavior of marine deposited clays, examined for the first time considering a sensitivity framework. Such an examination allows assessment of the effect of burial depth and cement incorporation on structure. This study further enables manipulation of the engineering properties and hence serves to develop the constitutive modeling of cement treated clays. Furthermore, a well-established relationship developed in shrinkage and compressibility of marine deposited clays will serve to optimize these two independent soil properties.

Key Words: Compression, Clay, Cementation, Sensitivity, Shrinkage, Structure

1. Introduction

The marine clay deposits addressed in this paper are mainly disseminated in the northern coast of Cyprus. Owing to variations in the engineering rock or depositional environment, marine deposited clays may demonstrate diverse characteristics. Geotechnical assessment of various sites at the Kyrenia region in Northern Cyprus revealed that intensive construction activity is occurring on the marine deposited Değirmenlik/Kythrea group clay formation that can be found at depths of 5–25 m [1].

These construction activities mainly involve soil excavation and disposal. From an environmental point of view, the dust emissions generated during excavation, transport, and disposal affect the people, environment, flora, and fauna around the region. Furthermore, the amount of excavated soil and the cost of transportation and handling can be substantial. Therefore, earthwork companies are disposing excavated soils over streams where such activity appears to cause floods. In the structural sense, construction on randomly disposed untreated Değirmenlik/Kythrea group clays cause problems with the structures owing to differential settlements. The most common solution is to transfer the excavated soil to stone quarries. However, when considering the distance to the quarries, this option causes traffic congestion, excessive CO_2 emission, and, consequently, additional project costs. The aforementioned problems can be reduced by optimizing the use of excavated soils to minimize both costs and the environmental impact. There are many possible solutions for managing excavated soil that can diverge on each individual project. Eras et al. [2] and Lafebre et al. [3] have proposed management options for excavated soils in order of preference: use on site, use in other projects, pretreated before use in other projects, store for later use, use as landfill cover, or dispose at landfill.

To mitigate structural failures and re-use the available soil, researchers have introduced additives to stabilize the existing soil. Catton [4] and Clough et al. [5] were among the earliest investigators of soil–cement use. The authors reported that the performance of soil–cement is complex and influenced by many aspects, such as the size, shape, and roughness of the soil particles; amount and type of cement; porosity; and curing time. More recently, the use of cement to increase the strength of cemented clays has been extensively investigated by Asano et al., Gallavresi, Kauschinger et al., Matsuo et al., Nagaraj et al., and Uddin et al. [6-11]. Lee et al. [12] proposed that, for a given type of cement mixed with a given type of cohesive soil, the unconfined compressive strength may be correlated with the water–cement ratio. However, Nagaraj et al. [10] suggested that the soil–cement ratio also affects the strength of the treated soil. Chew et al. [13] and Kamruzzaman et al. [14] studied the development of microstructure in cement treated Singapore marine clay by conducting Scanning Electron Microscopy (SEM), detecting an increase in the degree of flocculation at higher cement contents. Furthermore, Kamruzzaman et al. [14] conducted oedometer and undrained triaxial tests and reported that the incorporation of cement caused an increase in the preconsolidation pressure and a decrease in the swelling index of the clay.

It is a well-known phenomenon that change of moisture content can cause extensive volumetric changes in marine deposited clays. Foster [15] reported that because of the seasonal and environmental conditions, shrink-swell behavior is most apparent near ground surface. Furthermore, Fredlund [16] examined the engineering properties of expansive clays in the Saskatchewan region of Canada and concluded that the clays in this region are Ca (Calcium) Montmorillonite clays with high plasticity and swelling potential. Mitchell [17] and Murray [18] stated that mineralogical composition has an important effect on the swelling potential of the expansive soils. The authors mentioned that different clay minerals show different swelling potentials owing to changes in their structural and inter-layer bonding. Mitchell [17] further stated that smectite and vermiculites cause large volume changes as a result of wetting and drying.

Additionally, the mechanical properties of a soil have a significant role in the management possibility of an excavated soil. Therefore, an intensive study of subjected soil, considering well-established geotechnical theories, are fundamental to understanding the possibilities of soil reuse. The common practice in defining the effect of structure on the behavior of a soil is to compare the mechanically altered soil with the same soil in a reconstituted state. A reconstituted clay is defined by Burland [19] as one that has been thoroughly mixed at a water content equal to or greater than the liquid limit (w_L).

In their study of a constitutive model for structured clays, Baudet and Stallebrass [20] stated that the behavior of clays with a metastable structure is more complex because of destructuration. Coop and Cotecchia [21] suggested that the compression curve of an intact specimen may tend toward converging to the Intrinsic Compression Line (ICL), demonstrating a *metastable* structure that decreases with an increase in strain. Alternatively, authors reported that the compression curve may follow a line parallel to the ICL, highlighting the presence of *stable* elements of structure that do not degrade and lead to a constant stress sensitivity ratio. Furthermore, Baudet and Stallebrass [20] and Burland et al.

[22] have all suggested that the metastable elements of structure are more likely to be associated with bonding, whilst the stable elements are likely to result from the soil fabric. The authors also reported that separation of the individual effects of fabric and bonding on particular aspects of soils mechanical behavior is not possible. Therefore, the authors believe that soils will be performing in a stable and metastable condition simultaneously.

Hight et al. [23] investigated natural sample data from London Clay and concluded that the yield of the natural London Clay is poorly defined, with compression paths that continue to diverge from the ICL even at higher stresses. A study by Gasparre et al. [24] on London Clay revealed that there were clear differences in structure between the lithological units, with the compression paths for intact samples from the shallower units reaching states further outside the ICL than the deeper units. Tests on samples from different depths within the same lithological unit showed less variations, both in the location of the ICL and in the compression paths of the intact samples.

Although several studies were conducted on the compressibility of in-situ marine clays in the past, the investigation of the compression behavior of the properties of Cyprus clays are not addressed in the literature. The aims of this study, therefore, are to investigate the compressibility behavior of clays from the Değirmenlik/Kythrea group and the effects of cement incorporation on the one dimensional consolidation in terms of the sensitivity framework. This study also focuses on the effects of cement stabilization on structures and, more specifically, the influence of cement content on compression and shrinkage behavior. The results of treated and untreated marine deposited clays are then supported by microstructural analysis to gain an insight into the actual mechanism responsible for the enhancement of mechanical behavior.

2. Theoretical Background

Terzaghi [25] defined sensitivity, S_t, as the ratio, at the same void ratio, between the undrained strength of the undisturbed clay and the undrained strength of the reconstituted clay. The sensitivity is generally considered as the parameter symbolizing the differences of the microstructures of the natural and the reconstituted clays. The normalisation, using the void index (I_v) proposed by Burland et al. [22], removes the effect of soil composition or mineralogy and was used to highlight the effects of structure during compression.

The void index, I_v, is defined as Burland et al. [22]:

$$I_v = \frac{e - e^*_{100}}{e^*_{100} - e^*_{1000}} \quad (1)$$

Where: e is the void ratio of the soil. e^*_{100} and e^*_{1000} are the intrinsic void ratios corresponding to vertical effective stresses of 100kPa and 1000kPa respectively. Cc^* is the intrinsic compressibility and is defined as $e^*_{100} - e^*_{1000}$. Therefore, normalisation can be done by taking into account the slope and intercept of each clay, by introducing the I_v parameter. So, when the void ratio e is equal to e^*_{100}, $I_v = 0$, and when $e = e^*_{1000}$, $I_v = -1$. That means that all the Normal Compression Line (NCL) replotted from the e-logσ_v' into the I_v -logσ_v' plot passes through these two points, and thus define a unique line: the Intrinsic Compression Line (ICL).

Adapting the I_v normalisation proposed by the Burland et al. [22] cancels all the differences due to the intrinsic properties of the different reconstituted clays. Therefore, ICL represents a convenient reference line for the compression behaviour of clays. Any natural clay that plots above the ICL is deemed to have some form of structure. In addition to these studies, Cotecchia and Chandler [26] have explored that idea further, by re-plotting all data by Skempton and Petley [27] into a plot of void index, *Iv*, against logσ_v'. Authors found that the same pattern emerges, with NCLs plotting on the ICL when the clays are reconstituted (sensitivity ratio of 1), and natural clays plotting above it; the further from the ICL the higher their sensitivity as shown by Cotecchia and Chandler [26].

Further on the same authors introduced a new definition of sensitivity that use the yield stress instead of the undrained shear strength. Authors suggested that, on the basis of the data reported in their studies, the stress sensitivity (S_t) is, for all practical purposes, numerically equal to the strength sensitivity (S_σ). The stress sensitivity introduced the parameter $S_\sigma=\sigma`_y/\sigma^*_e$ (where $\sigma^*_e$ is the equivalent pressure on the ICL and $\sigma`_y$ is the equivalent pressure, taken on the ICL for the void ratio of the natural clay at gross yield), defined as the stress sensitivity ratio, to quantify the influence of microstructure on the size of the gross yield pressures.

The Sensitivity framework Cotecchia and Chandler [26] link the volumetric behaviours and shearing. It is important to mention that this implies that the degree of structure, measured in terms of yield stress and in terms of shear strength, must be similar, therefore the shapes of the State Boundary Surfaces (SBS) of the intact and the reconstituted soils must also be similar in shape. The SBS for the intact natural clay will be larger, by a factor of magnitude equal to the sensitivity where such finding is important for modelling purposes.

3. Geological Background

3.1. Site Investigation and Location

Block samples were collected from the AD-G site, located in the Kyrenia District, northern coast of Cyprus, located at Grid Reference 535633E, 3910238N (Figure 1). The blocks were obtained during the excavation phase at a depth of approximately 15 m. The site dips towards the sea, with a slope angle of approximately 8°. The slope is bound at the top by fields and at the bottom by the Mediterranean Sea. Eight undisturbed samples were also recovered from boreholes at six different sites in the Kyrenia region, as shown in Figure 1. Hence, the investigated area covers a span of 10 km on the north shore of the Cyprus island.

Atalar [28] studied the clays of Cyprus and reported that the Degirmenlik group clays occurred during the post Cretaceous period as a result of the alteration of the Troodos ophiolite and the pelagic sedimentary cycles that followed. The author concluded that the calcium carbonate content of the marls originated from the limestones and dolomites of the Kyrenia zone and the chalks of the South Cyprus zone, and has a considerable part that is biogenic in origin.

Furthermore, Palamakumbura [29] noted that the initial emergence of the Kyrenia Range began during the Pliocene Epoch and resulted in a non-marine mountain range, surrounded by a shallow-marine environment. Additionally, the author added that the base of the sequence comprises a thick bedded carbonate deposit containing beds rich in either benthic and planktonic foraminifera or calcareous red algae. He also mentioned that the basal carbonate deposit is overlain by a packstone deposit comprising reworked carbonate and siliciclastic material with cross-stratification, laminations, and trough cross-bedding. The composition of the carbonate material includes echinoids, bivalve fragments, benthic foraminifera, red algae, bryozoan, and ostracods.

3.2. Site and Sampling

The block sampling process was carefully organized, and with the help of an excavator a trench was made. The excavator did not excavate closer than 300 mm to the sample sides. Great attention was paid to limit the disturbance to samples, and the final stage of the excavation was conducted with a pneumatic clay spade, soil saw, and manual clay spades. Blocks were formed, wrapped with cling film, and waxed to retain the moisture content. The samples were then placed into wooden boxes and transferred to the Soil Laboratory.

Prior to the start of the project, rotary core samples were recovered using a triple barrel rotary corer. Extracted samples were visually examined, cut into pieces of 15-20 cm, and those disturbed were discarded. The selected samples (considered undisturbed) were wrapped in several layers of cling film, waxed, and stored in the humidity chamber together with block samples.

4. Materials and Methods

4.1. Materials

To characterize the tested specimens, the specific gravity, Atterberg limits, and particle size distribution were determined. This was vital for the additional analysis conducted in the study. Preliminary tests were repeated for every oedometer specimen to assess the consistency of the used material.

In this study, the Atterberg limits were conducted in accordance with ASTM D4318-17e1 [30]. A summary of the properties of the clay sample used in this study is presented in Table 1. It can be seen that for all tested specimens the liquid limit varies in a narrow range from 40% to 54%, and the plastic limit varies over a narrow range from 21% to 26% indicating homogeneity of the studied formation. It was also observed that the natural moisture content on site is smaller than the liquid limit and varies between the range from 17.10% to 28.48%. This difference in natural moisture content for the studied formation is mainly controlled by the clay content, particle size, and stratification characteristics of the sampling locations. The liquid limit and plasticity index values are increased accordingly with the increase in the true stratigraphic depth of the sampling location. Depending on the index properties, the clay sample used in this study is classified as an inorganic clay of medium (CL) to high plasticity (CH), according to the Unified Soil Classification System (USCS) ASTM D2487-17 [31]. Where USCS is most commonly used soil classification system to describe the texture and grain size of a soil.

Furthermore, the small pycnometer method was used in accordance with ASTM D854-14 [32] to define the specific gravity of the selected samples.

Figure 2 shows the soil grading curves of the different samples used in this study. Wet sieving was used to separate the soil into its size fractions. Any soil passing through the finest mesh (0.063 mm) was subjected to a sedimentation test to determine the distribution down to a particle size of 0.002 mm. The particle size distribution curves indicated that the specimens AD, C, and AC have similar sizes, and a clay size and fine silt content of approximately 60% and 35%, respectively. Sample DKS has a slightly lower clay content, approximately 50%, with 20% fine silt and approximately 28% medium silt.

The SEM of undisturbed Değirmenlik/Kythrea clay is shown in Figure 3. The particles of marine deposited clay are typical of hollow and disc forms of coccolithic (nannofossil) origins and this is clearly shown in Figure 3, a SEM of undisturbed Değirmenlik/Kythrea clay. This is an indication of the high calcium carbonate content of Değirmenlik/Kythrea clay. Moreover, X-ray spectroscopy analysis has shown that such clay is very rich in silica, alumina, and calcium. Furthermore, X-ray diffractometry of studied clay verified the findings of SEM and presented in Figure 4. The semi-quantitative analysis indicated that the Calcite (C) with an amount being approximately 40% is the major mineral of the used clay. The other minerals are Quartz (Q), Montmorillonite (smectite) (M), Chlorite/Kaolinite (Ch) and Feldspar (F) ranging from 10% to 15 %, respectively. Illite (I) with an estimated amount of 5% is the other clay mineral observed.

Ordinary Portland Cement (PC) grade 42.5 (ASTM C150M-18[33]) was used for the purpose of stabilization. The Blaine fineness and specific gravity of the cement are 289 m^2/kg and 3.12, respectively.

4.2. Sample Preparation

In this study, marine deposited Değirmenlik/Kythrea group clays from seven different sites have been tested in reconstituted and in-situ states. Specimens from the AC-G site have been subjected to cement stabilization in a slurry state.

Therefore, in this study, samples were remolded to a water content varying between 1 w_L and 1.5 w_L. Such variations were proposed by Burland [19] intentionally to study the effects of the initial water content on the position and slope of the intrinsic normal compression line.

After increasing the moisture content to the desired percentage and thoroughly hand mixing the sample to a uniform slurry state, the sample was transferred to an oedometer ring where the side of the porous stones in contact with the soil was covered with a wet filter paper. Therefore, the porous stone and filter paper were also acting as a base to facilitate the transfer of the slurry into the ring.

The in-situ specimens were carved from block and rotary samples by pushing the ring and trimming the specimens with a palette knife, until the sample rose above the top portion of the ring. This process was performed with care to avoid sample disturbance. After the sample was protruding from the top and bottom of the ring, it was cut from the block and the edges trimmed to obtain a perfect cylinder. The excess from the trimming process was used for determining the moisture content and calculating the initial void ratio of the specimens.

For the cement stabilized mixture, dry powdered clay and Portland cement were weighed separately and dry mixed to attain a uniform consistency. Water was then added to the specimen and mixed until a homogeneous paste was obtained. The chosen cement percentages were 1%, 3%, 5%, and 7% of the soil dry mass. The specimen was inserted in the oedometer ring by using the procedure previously described for slurry. Samples were then cured in a humidity chamber at 22±2 $C°$ and a relative humidity of 96% for one day.

In accordance with the results of the above studies, the free shrinkage behaviors of specimens from the AD-G site have been assessed. Samples were prepared in a reconstituted state and transferred in split molds. For all monitored specimens, three samples were prepared in dimensions of 150 mm diameter and 45 mm height. Specimens were brought to the desired moisture content, approximately 65%, which is 1.5 w_L. Cement was hand mixed in a dry condition at 1%, 3%, 5%, and 7% of the dry weight of the soil to achieve a homogeneous distribution, where later the required water content was added, and the samples were thoroughly mixed and transferred to molds.

4.3. One Dimensional Compression Testing

The one dimensional compression test of the prepared specimens has been performed in accordance to ASTM D2435/D2435M-11[34]. The initial dimensions of the sample were determined by measuring the internal diameter and height of the oedometer ring and by comparing it with the reference height of a dummy sample. The slurry samples were assumed to be fully saturated to calculate the initial void ratio from the initial dimensions and the initial solid weight. Calculations based on this method were found to correspond very well with the void ratio determined from the initial water content. A slightly larger discrepancy was found when the initial void ratio was back-calculated from the final water content. For each conducted test, the values of the initial void ratio calculated from the suggested methods were compared and any inconsistent values were discarded. An average of the measured values provided the initial void ratio used for the analysis. The variation of e_i for the four methods was determined to be ±0.01 to 0.02. To ensure the repeatability of test and get a reliable result of compression, each test in Table 1 were repeated at least two times. The specimens which shows more the ±0.04 variation of void ratio at specific effective stress were further repeated up until ensuring required variation limit.

4.4. Shrinkage

The literature review performed revealed that there is no single technique that can be determined to be the best to monitor specimen drying. Therefore, the authors decided to use a technique that has been successfully applied to monitor the shrinkage of London clay reinforced with fibers [35]. All samples were allowed to air dry at room temperature for approximately 30 days. During this period, the weight was measured regularly, together with six measurements of the diameter and four measurements of the height of the sample, in different positions on the sample. To improve the accuracy, all height and diameter measurements were performed at the same points on each sample. In addition, photographs of the specimens have been taken from different angles at similar intervals. These were used for a dimension measurement and for a qualitative analysis of shrinkage and crack development.

4.5. Microstructural Tests

To analyze the microstructural development of the cemented clays, SEM was conducted at the end of the consolidation process on undisturbed and cemented samples of Değirmenlik/Kythrea clay. The SEM was performed using a Jeol JSM-6480LV high-performance, Variable Pressure Analytical Scanning Electron Microscope with a high resolution of 3.0 nm, along with an Energy Dispersive System (EDS) system. For the analysis, small dried pieces of test specimens were glued to aluminum stubs. A coat of silver paint was used to ensure electrical contact between the stud and the sample before a gold coating was applied to the sample, and the samples were then tested. The SEM images were taken at different levels of magnification in the range of 4000x to 5500x. X-ray powder diffraction (XRD) analysis using a Cu X-ray tube was performed on powdered samples, and patterns were obtained by scanning at 0.2° (2θ) per min and at steps of 0.04° (2θ). The voltage and current used in the XRD analysis were set at 40 kV and 30 mA, respectively.

5. Results and Discussions

5.1. Compression Behavior

The compression test results of the reconstituted and intact marine deposited clays are shown in Figure 5. Although the samples are from the same lithological units, they have been collected from different depths, and the increase in stress level lead the ICLs of the reconstituted specimens to converge at the larger pressures. In contrast, the compression curves of the intact samples, also collected from various depths, are fairly unique for each lithological unit, as is also shown in Figure 5. The compression curves of the intact specimens curve gently downwards at higher pressures, producing no single clear yield point, similar to the behavior of London Clay shown by Gasparre et al. [24] and other stiff clays from the UK, shown by Hosseini Kamal et al. [36]. According to both authors, this is due to the gradual destructuration as the stress increases. It is clear that the initial state of the tested specimens reflects the in-situ void ratio, which is controlled predominantly by plasticity, depth of burial, and grading. It can be seen that the compression curves defined by more plastic specimens (DKS and EA) fall above those that have lower plasticity (AD and L). Furthermore, the intact specimens from AD and L have the lowest in-situ void ratio mainly because of the burial depths (15 and 20 m, respectively) that fall below the DKS and EA specimens from shallower depths (7.5 and 9 m, respectively). It should be noted that this is also reflected in the specimens' intact compressibility. The results reported in this paper, as well as the results stated in Burland et al. [22], show that the intact state deposition is emerged above the ICL. It can be seen that the bond strength in one dimensional compression does not diminish as the applied stress exceeds the yield stress level. This has been the case in DKS specimens, which are deposited in depths shallower than all other specimens and have a medium silt content in the grain size distribution. Therefore, the compression curves of those specimens indicate that the behavior is not only affected by the nature of the samples, it is also affected by the structure.

The compression behavior of the reconstituted specimens, together with the cement treated specimens, are shown in Figure 6. The cement content used for the treatment were 1%, 3%, 5%, and 7% by dry weight of clay. Specimens treated with 1% cement show similarities to the intrinsic specimens, and the compression behavior is not significantly enhanced. The most apparent effect of cement treatment on the compression behavior is the increase observed in the yielding stress. It must be noted that the increase in cement content resulted in a further increase in yielding stress. As a result of the development of this cementation-induced yielding, the compression curves of stabilized clay are shifted to higher void ratios and are able to resist almost 10–15 times the vertical effective stress sustained by the reconstituted clay.

The results shown in Figures 5 and 6 indicate that in-situ specimens are exhibiting a stable structure as they are following a parallel or same line of ICL following yielding. As cemented specimens are bending towards the ICL, they exhibit a *metastable* structure. It is already reported in theoretical background that the *metastable* structure of cemented specimens are due to the bonding introduced by the cementation. It can be observed that once a particular stress, proportional to the cement amount, is reached, the cement bonds start breaking and an abrupt increase in compressibility is seen. The results obtained appear to show that the compression curves are trending towards the ICL; however, larger pressures would be required to show that the samples would reach and follow the ICL. The in-situ samples, however, show a different behavior dominated by the fabric rather than bonding, which is responsible for the stable structure.

The coefficient of volume compressibility, m_v, of the intact, reconstituted, and cemented specimens are shown in Figure 7. It can be seen that, despite the variations in the initial state of the specimens, the increase in the vertical effective stresses results in a decrease in the coefficient of volume compressibility. At low stresses, the effect of cement addition is more visible as the increase in cement content lead to a less compressible state. Samples that are 1% cemented and reconstituted have a more gradual change in the coefficient of compressibility with no rapid changes in the curvature of the compression line that reflects a clear yield stress. However, cemented samples with 3%, 5%, and 7% cement show a coefficient of compressibility that is constant with the increase in the load, until a compression yielding is experienced and the compressibility decreases. For stresses higher than 1000 kPa, the observed differences in compressibility diminishes and the coefficients of volume compressibility tend to become identical. The addition of cement seems to have correlated effects, which suggest that both the cement content and nature of the clay have a significant influence on the compression behavior.

The oedometric compression curves of all specimens tested in this study are normalized using the void index (Iv) and are shown in Figure 8. The results indicate that the effect of structure on the compression behavior is influenced by burial depth. The specimens tested from shallower burial depths cross the ICL continue to plot well above it, then gradually decline at large stresses. However, specimens from greater depths plot close and parallel to the ICL and respond with gradual yield. Such observations reveal that the effect of structure on the compression behavior of the intact material decreases with an increase in burial depth, which is in agreement with previous findings [23,37,38].

The stress sensitivity ratios for all intact and cemented specimens examined in this study are calculated according to the methodology proposed by Cotecchia and Chandler [26], and the values are listed in Table 2. It can be observed that Figure 8a indicates values of $S\sigma > 1$ for intact and cemented specimens. To further visualize the influence of the burial depth, Figure 9 demonstrates the stress sensitivity ratio with varying depth. The stress sensitivity ratios for all intact specimens show significant variation in the effects of structure on the compressibility with depth. Furthermore, the cement treated reconstituted specimens appear to directly influence the stress sensitivity ratio.

The results reported in this paper have important practical implications as they provide significant knowledge about the compressibility behavior of Cyprus marine deposited clays, for the first time. The compressibility behavior of marine deposited clays, examined considering the sensitivity framework, enable the assessment of the effect of burial depth on structure. The influence of cement incorporation on the marine deposited clays enables manipulation of the engineering properties and hence serve the development of the constitutive modeling of cement treated clays.

5.2. Shrinkage Behavior

The increasing levels of cement incorporations on the free shrinkage behavior of the studied soils are shown in Figure 10. The volume of the specimens was normalized by dividing the current volume of specimen *V(c)* by the initial volume of specimen *V(i).* The graph shows that the increase in the cement content enhances the soil resistance to volumetric changes. It can be seen that in untreated samples immediate reductions in volume have been monitored in 14 days. The treated samples, however, mainly experienced smaller volume reduction with the increase in cement content.

The influence of cement incorporation on axial, radial, and volumetric shrinkage are shown in Figure 11. The shrinkage percentage shown in the graph indicates the final average reduction of all tested specimens with respect to cement content. The results shown indicate that a systematic increase in the cement content resulted in a systematic decrease in shrinkage in both the axial and radial directions. It must be noted that specimens in the radial direction experience a higher shrinkage compared to those in the axial directions. Specimens with cement content higher than 1% do not seem to be dramatically affected by the shrinkage in the axial direction. Furthermore, the incorporation of 7% cement does not seem to further influence the shrinkage behavior of specimens examined herein.

Figure 12 shows pictures of the specimens studied in this paper that are classified according to the cement content and the elapsed time after mixing. The shrinkage trends observed in the photos are in good agreement with the change in volumetric shrinkage strain shown in Figure 10.

The results clearly show that the use of cement treatment in these clays significantly reduces the volumetric changes experienced during drying. This behavior is mainly attributed to the formation of ettringite, namely calcium sulfoaluminate, that develops as a result of the chemical reaction between cement and clay minerals. It is a well-known fact that gypsum is purposely added to Portland cement to regulate early hydration reactions. This incidence is necessary to prevent flash setting of cement-based materials. Incorporation of gypsum also improves strength development and reduces the drying shrinkage of these materials. The formation of ettringite fills the pores in the matrix, resulting in a significant reduction in the total volume of pore space. Ettringite formation and, consequently, the decrease in the void space that results in more consolidated clay matrix therefore play a key role in reducing the volumetric changes of these cement treated specimens.

5.3. Microstructure Influence

The SEM analyses conducted on the 5% treated marine deposited clays at the end of consolidation process are shown in Figure 13. It can be seen that the process of cement hydration resulted in the formation of needle-like crystals, calcium silicate hydrate (CSH), between the particles. These crystals have a high aspect ratio with a maximum diameter of 0.3 μm and a length of 5 mm. High aspect ratios revalidate the formation of CSH needles in the matrix that is responsible for the increase in yielding stress in one dimensional compression. The Energy-dispersive X-ray spectroscopy (EDX) analysis, shown in Figure 14, indicates that these crystals contain considerable amounts of aluminum, calcium, and sulfide ions in comparison to the soil particles. Thus, these crystals could form calcium-alumino-monosulfohydrate and further form ettringite as a result of the reaction between

C_3A (one of the compounds forming Portland cement) with sulfate and aluminum, both present in the specimens, according to the EDX analysis. Moreover, Figure 15 shows the XRD pattern of 5% cement treated clay contains the clay minerals of Calcite (C), Quartz (Q), Montmorillonite (smectite) (M), Chlorite/Kaolinite (Ch), Feldspar (F) and Illite (I) ranging between same percentages as reported previously. Furthermore, peaks corresponding to predominantly ettringite (E) and inconsiderable amount of CSH are appearing that confirms the development of ettringites.

It must be noted that in the case of slurry state clays, the formation of ettringite is easier owing to the high void ratio of the specimens. It is also known that ettringite formation causes expansion in the matrix. The results reported in this paper indicate that the crystallization of ettringite generates considerable volumetric expansion, which not only reduces the compressibility, it also increases the shrinkage resistance of the cement treated clays.

A relationship between the stress sensitivity ratio and the normalized volume shrinkage strain is plotted in Figure 16. It can be observed that there is a linear relationship between the two plotted values. The increase in cement content appears to be responsible for the decrease in shrinkage and, accordingly, the increase in the stress sensitivity ratio. This can be attributed to the bonding and formation of ettringite in the pores of the sample, owing to the cement hydration further restricting the compression of the cemented specimens. Such an aspect seems to be eroded with the increase in vertical stress by breaking the bonds induced by cementation. The authors believe that this behavior can be attributed to the *metastable* structure induced by the bonding created with the addition of cement.

5 Conclusions

The following conclusions can be drawn based on the results of this study:

- The most apparent effect of cement treatment on compression behavior is the increase in cement content that resulted in a further increase in yielding stress.
- In-situ specimens exhibit a stable structure where cemented specimens bend towards the ICL and exhibit a *metastable* structure. Once the artificial preconsolidation pressure is exceeded, the bonds between the particles break, resulting in a sudden increase in compressibility. However, for the in-situ specimens, it is the fabric that is responsible for the stable structure.
- At low stresses, the effect of cement addition on the coefficient of volume compressibility is more predominant where the increase in cement content led to a less compressible state. However, for stresses higher than 1000 kPa, the observed differences in compressibility diminish.
- The stress sensitivity ratios for all intact specimens show a significant variation in the effects of structure on compressibility with depth. Furthermore, the cement treated reconstituted specimens appear to directly influence the stress sensitivity ratio.
- The influence of the cement incorporation on the shrinkage indicates that a systematic increase in the cement content resulted in a systematic decrease in the shrinkage in the axial and radial directions. The shrinkage of the specimens in the radial direction is higher than in the axial direction.

- A linear relationship established between the stress sensitivity ratio and the normalized volumetric strain caused by shrinkage. The increase in cement content is responsible for the decrease in shrinkage and the increase in the stress sensitivity ratio. The author believes that this behavior can be attributed to the *metastable* structure induced by bonding established owing to cementation.
- SEM analysis revealed that the ettringite crystals demonstrate considerable volumetric expansion, which not only reduces the compressibility, it also increases the shrinkage resistance of cement treated clays. Furthermore, this has been attributed to ettringite development in pore spaces owing to cement inclusion that restricts compressibility, leading to a reduction in settlement.
- Reuse of unsuitable soil reduces the environmental and financial impacts caused by disposal. By bringing the unsuitable soil to a slurry state and using cement stabilization will enable the use of the material on site. Furthermore, this process does not require any specific tool, which makes the process convenient.

6 Funding

This research did not receive any specific grant from funding agencies in the public, commercial, or not-for-profit sectors.

7 Acknowledgement

Author greatly appreciates the discussions and help of Prof. Dr. Nilo C. Consoli from Universidade Federal do Rio Grande do Sul. Author also thanks his graduate student Mr. Mohamad Hanafi and Mr. Doğan Gülaboğlu for their support during the laboratory experiments.

8 References

1 Robertson AHF, Parlak O, Ünlügenç UC (2013) Geological Development of Anatolia and Easternmost Mediterranean Region. Geological Society, London.

2 Eras JJC, Gutiérrez AS, Capote DH, Hens L, Vandecasteele C (2013) Improving the environmental performance of an earthwork project using cleaner production strategies. J Clean Prod 47:368-376.

3 Lafebre, H, Songonuga O, Kathuria, A (1998) Contaminated soil management at construction sites. Practice Periodical of Hazardous, Toxic, and Radioactive Waste Management, Am Soc Civ Eng 2(3):115-119.

4 Catton MD (1962) Soil-cement technology—A résumé. Research and Development Laboratories of the Portland Cement Association, Portland, OR.

5 Clough GW, Sitar N, Bachus RC (1981) Cemented sands under static loading. J Geotech Eng Div 107(6):799-817.

6 Asano J, Ban K, Azuma, K, and Takahashi, K (1996) Deep mixing method of soil stabilization using coal ash. IS Tokyo ’96, 2nd International Conference on Ground Improvement Geosystems, Tokyo, 393-398.

7 Gallavresi F (1992) Grouting improvement of foundation soils. Grouting, soil improvement and geosynthetics. ASCE, New York, 1-38.

8 Kauschinger JL, Hankour R, Perry, EB, Kauschinger L, Joseph M (1992) Methods to estimate composition of jet grout bodies. Grouting, soil improvement, and geosynthetics: Proceeding of the conference (geotechnical special publication), 1:194-205.

9 Matsuo T, Nisibayashi K, Hosoya Y (1996) Studies on soil improvement adjusted at

low compressive strength in deep mixing method. IS Tokyo ’96, 2nd International Conference on Ground Improvement Geosystems, Tokyo, 521-526.

10 Nagaraj TS, Miura N, Yaligar PP, Yamadera A (1996) Predicting strength development by cement admixture based on water content. IS Tokyo ’96, 2nd International Conference on Ground Improvement Geosystems, Tokyo, 431-436.

11 Uddin K, Balasubramaniam AS, Bergado DT (1997) Engineering behavior of cement-treated Bangkok soft clay. Geotech Eng 28(1):89-119.

12 Lee, FH, Lee Y, Chew SH, Yong KY (2005) Strength and modulus of marine clay-cement mixes. J Geotech Geoenvironmental Eng 131(2):178-186.

13 Chew SH, Kamruzzaman AHM, Lee FH (2004) Physicochemical and engineering behavior of cement treated clays. J Geotech Geoenvironmental Eng 130(7):696-706.

14 Kamruzzaman AH, Chew SH, Lee FH (2009) Structuration and destructuration behavior of cement-treated Singapore Marine Clay. J Geotech Geoenvironmental Eng 135(4):573-589.

15 Foster MD (1954) The relation between composition and swelling in clays. Clays Clay Miner 3:205-220.

16 Fredlund DG (1975) Engineering properties of expansive clays. shallow foundations on expansive clays. Seminar on shallow foundations on expansive clays, 27-28 October 1975, Regina, Saskatchewan.

17 Mitchell JK (1976) Fundamentals of soil behavior. John Wiley & Sons Inc, New York.

18 Mitchell JK (1976) Fundamentals of soil behavior. John Wiley & Sons Inc, New York.

19 Burland JB (1990) On the compressibility and shear strength of natural clays. Géotechnique 40(3):329-378.

20 Baudet B, Stallebrass S (2004) A constitutive model for structured clays. Géotechnique 54(4):269-278.

21 Coop MR, Cotecchia F (1995) The compression of sediments at the archaeological site of Sibari. 11th European conference on soil mechanics and foundation engineering, Danish Geotechnical Society, Copenhagen, 19-26.

22 Burland JB, Rampello S, Georgiannou VN, Calabresi G (1996) A laboratory study of the strength of four stiff clays. Géotechnique 47(2):390-390.

23 Hight DW, Gasparre A, Nishimura S, Minh NA, Jardine RJ, Coop MR (2007) Characteristics of the London Clay from the Terminal 5 site at Heathrow Airport. Géotechnique 57(1):3-18.

24 Gasparre A, Nishimura S, Coop MR, Jardine RJ (2007) The influence of structure on the behaviour of London Clay. Géotechnique 57(1):19-31.

25 Terzaghi K (1944) Ends and means in Soils Mechanics. Engineering Journal(Canada)ASTM 27, 608.

26 Cotecchia F, Chandler RJ (2000) A general framework for the mechanical behaviour of clays. Géotechnique 50(4):431-447.

27 Skempton AW, Petley DJ (1970) Ignition Loss and other Properties of Peats and Clays from Avonmouth, King's Lynn and Cranberry Moss. Géotechnique 20(4): 343–356.

28 Atalar C (2011) A review of the origin and properties of the soils of Nicosia, Cyprus. Int J Geotechnical Eng 5(1):79-86.

29 Palamakumbura RN (2015) Sedimentary response to the tectonic uplift of the Kyrenia Range, Northern Cyprus, in its Eastern Mediterranean tectonic setting. The University of Edinburgh.

30 ASTM (2017) Standard Test Methods for Liquid Limit, Plastic Limit, and Plasticity Index of Soils, ASTM D4318-17e1, ASTM International, West Conshohocken, PA.

31 ASTM (2017) Standard Practice for Classification of Soils for Engineering Purposes (Unified Soil Classification System), ASTM D2487-17, ASTM International, West Conshohocken, PA.

32 ASTM (2014) Standard Test Methods for Specific Gravity of Soil Solids by Water Pycnometer, ASTM D854-14, ASTM International, West Conshohocken, PA.

33 ASTM (2018) Standard Specification for Portland Cement, ASTM C150/C150M-18, ASTM International, West Conshohocken, PA.

34 ASTM (2011) Standard Test Methods for One-Dimensional Consolidation Properties of Soils Using Incremental Loading, ASTM D2435/D2435M-11, ASTM International, West Conshohocken, PA

35 Ekinci A, Ferreira PMV (2012) Effects of fibre reinforcement in the shrinkage behavior of compacted clay. 3rd International Conference on New Developments in Soil Mechanics and Geotechnical Engineering, Near East University, Nicosia, North Cyprus, 28-30.

36 Hosseini Kamal R, Coop MR, Jardine RJ, Brosse, A (2014) The post-yield behaviour of four Eocene-to-Jurassic UK stiff clays. Géotechnique 64(8):620-634.

37 Chandler RJ, Cotecchia F (1997) The influence of structure on the pre-failure behaviour of a natural clay. Géotechnique 47(3):523-544.

38 Gasparre A, Coop MR (2008) Quantification of the effects of structure on the compression of a stiff clay. Can Geotechnical J 45(9):1324-1334.

Table 1. Sample and Index Properties of Tested Specimens.

Specimen	Sampling Method	Depth	Testing Condition[a]	Void Ratio[b]	W_o[c]	*Gs*	*CF*	w_L	*PL*	*PI*	*A*[d]	*USCS*
		m			%	g/ml	%	%	%	%		
AD-G-REC-A	BLOCK	15.0	R	1.63		2.61	55	40	21	19	0.35	CL
AD-G-INSITU-A-15m	BLOCK	15.0	I	0.42	18.40	2.61		40	21	19		CL
AD-G-INSITU-B-15m	BLOCK	15.0	I	0.42	17.10	2.61		40	21	19		CL
EA-G-REC-A	SPT-UD	9.0	R	1.4		2.65	52	47	22	25	0.48	CH
EA-G-INSITU-9m	SPT-UD	9.0	I	0.54	17.44	2.65		47	22	25		CH
EA-G-INSITU-7. m	SPT-UD	7.5	I	0.71	18.80	2.65		42	21	21		CL
DKS-G-REC-A	SPT-UD	10.5	R	1.56		2.61	58	53	25	28	0.48	CH
DKS-G-INSITU- m	SPT-UD	9.0	I	0.78	23.94	2.70		53	25	29		CH
DKS-G-INSITU-7.5m	SPT-UD	7.0	I	0.72	23.17	2.70		54	26	29		CH
DKS-G-INSITU-10.5m	SPT-UD	10.5	I	0.81	26.45	2.70		53	23	30		CH
AV-G-REC-A	SPT-UD	9.0	R	1.64		2.65	50	46	23	23	0.45	CL
AV-G-INSITU-9m	SPT-UD	9.0	I	0.66	19.53	2.65		46	23	23		CL
C-G-REC-A	SPT-UD	11.0	R	1.29		2.70	58	46	26	20	0.34	CL
C-G-INSITU-11m	SPT-UD	11.0	I	0.86	28.48	2.70		46	26	20		CL
L-G-INSITU-20m	SPT-UD	20.0	I	0.52	22.50	2.61	54	45	25	20	0.37	CL
AC-G-INSITU-10.5m	SPT-UD	10.5	I	0.65	18.10	2.61	57	45	23	22	0.38	CL
AC-G-CEMENT 1%	SPT-UD	10.5	R	1.57		2.62						
AC-G-CEMENT 3%	SPT-UD	10.5	R	1.58		2.63						
AC-G-CEMENT 5%	SPT-UD	10.5	R	1.6		2.64						
AC-G-CEMENT 7%	SPT-UD	10.5	R	1.61		2.65						

Note: [a] I – In situ, R - Reconstituted, [b] Void ratio before 1-D compression test, [c] Natural moisture content at site, [d] A – Activity
CL- Inorganic clays of low to medium plasticity, gravelly clays, sandy clays, silty clays, lean clays.
CH – Inorganic clays of high plasticity, fat clays.

Table 2. Stress Sensitivity of In-situ and Cemented Specimens.

LOCATION		SENSITIVITY		
	Depth	$\sigma`_e$	$\sigma`_y$	S_σ
	m	kN	kN	
AD-G-INSITU-A-15m	15	400	850	2.13
AD-G-INSITU-B-15m	15	400	950	2.38
EA-G-INSITU-9m	9	400	800	2.00
EA-G-INSITU-7.5m	7.5	400	1050	2.63
DKS-G-INSITU-10.5m	10.5	400	870	2.18
DKS-G-INSITU-7.5m	7	400	1300	3.25
DKS-G-INSITU-9m	9	400	1300	3.25
AV-G-INSITU-9m	9	400	1150	2.88
C-G-INSITU-11m	11	400	950	2.38
AC-G-INSITU-10.5m	10.5	400	850	2.13
L-G-INSITU-20m	20	400	744	1.86
AC-G-CEMENT 1%	REC	400	600	1.50
AC-G-CEMENT 3%	REC	400	850	2.13
AC-G-CEMENT 5%	REC	400	1400	3.50
AC-G-CEMENT 7%	REC	400	1600	4.00

Figures

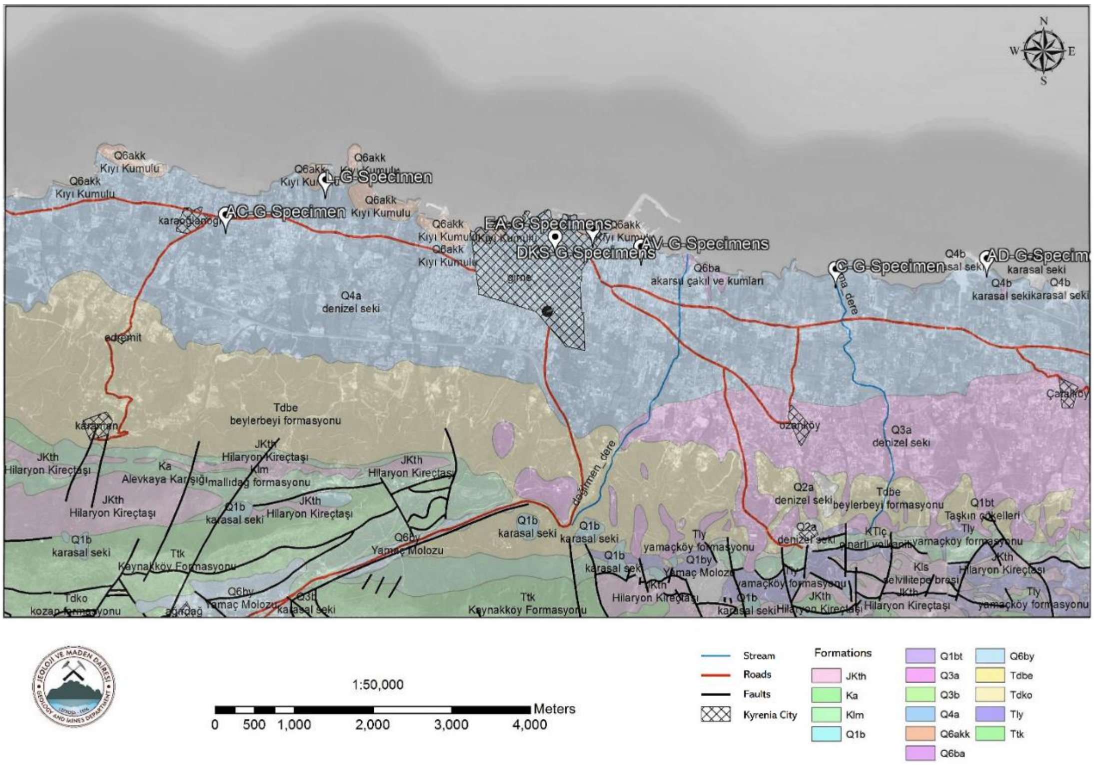

Fig. 1. Surface geology of the specimen locations (Geology and Mines Department).

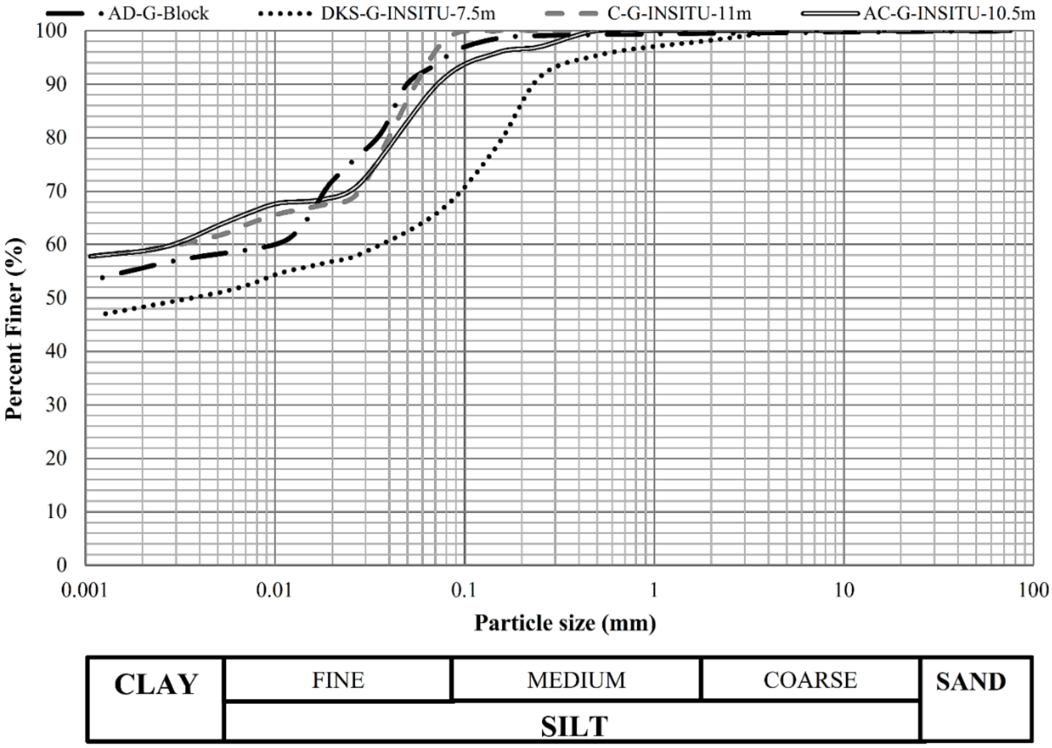

Fig. 2. Grain size distribution curves of specimens from various sites.

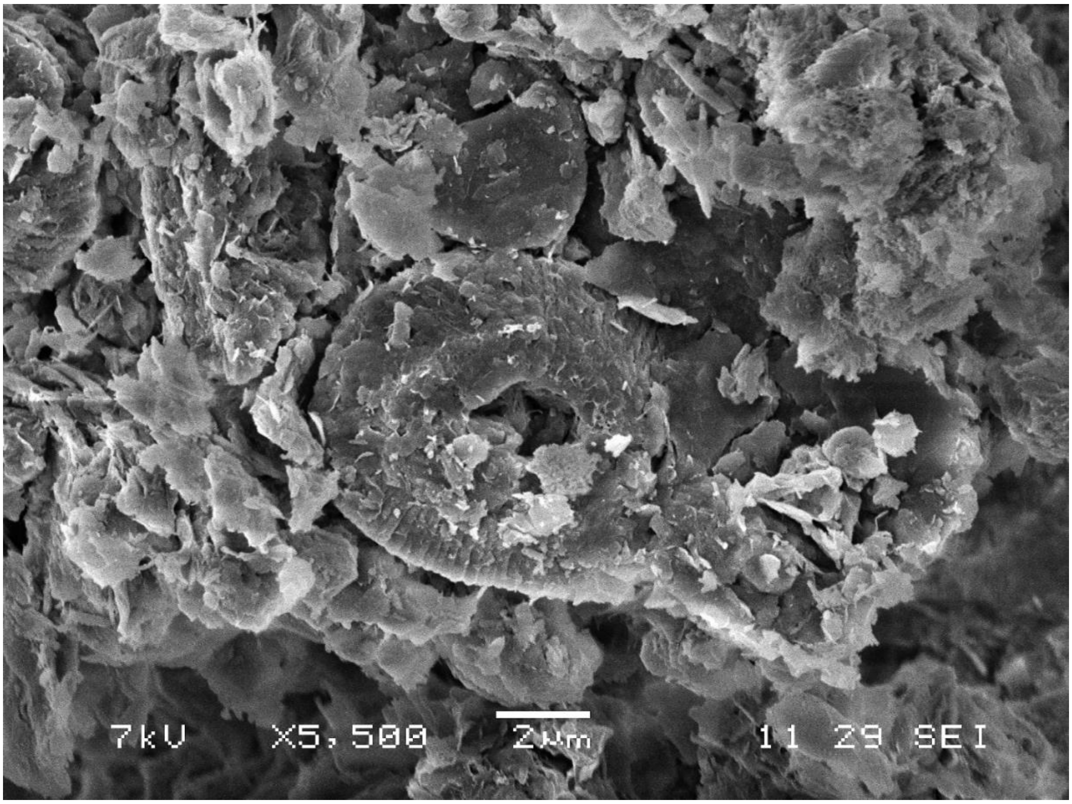

Fig. 3. Scanning electron micrographs of undisturbed Değirmenlik/Kythrea clay.

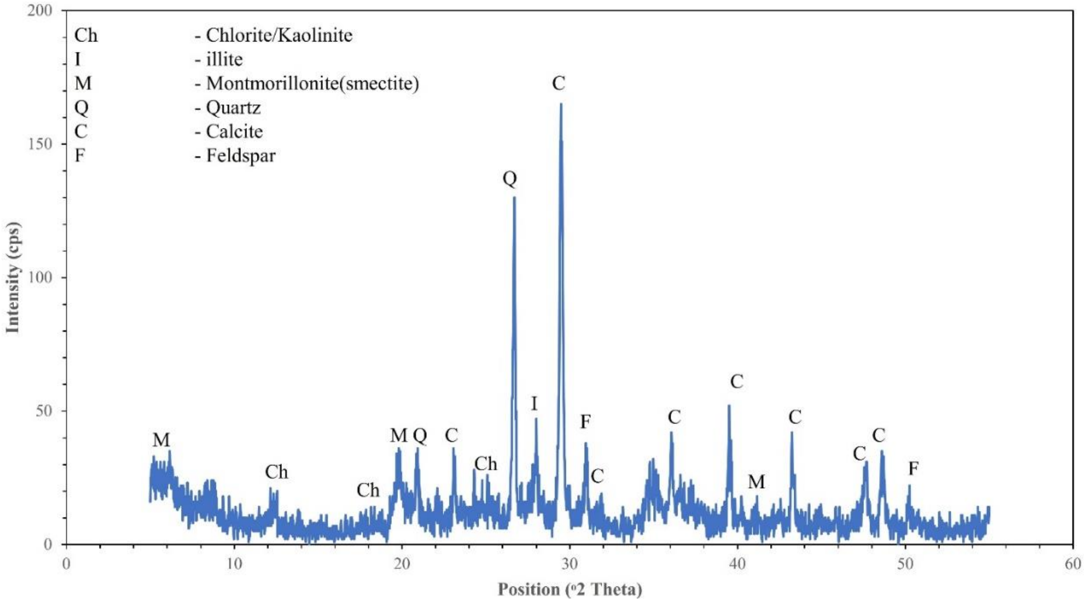

Fig. 4. X-ray diffraction of studied clay specimen.

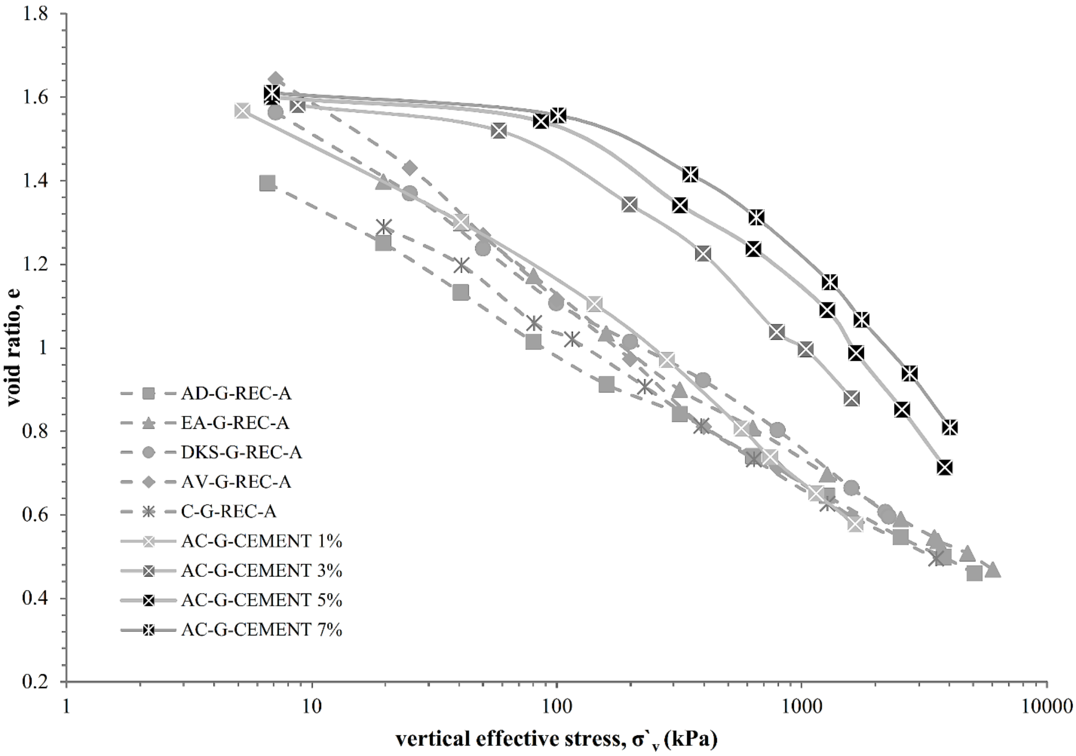

Fig. 5. One dimensional compression of undisturbed and reconstituted Değirmenlik/Kythrea clays.

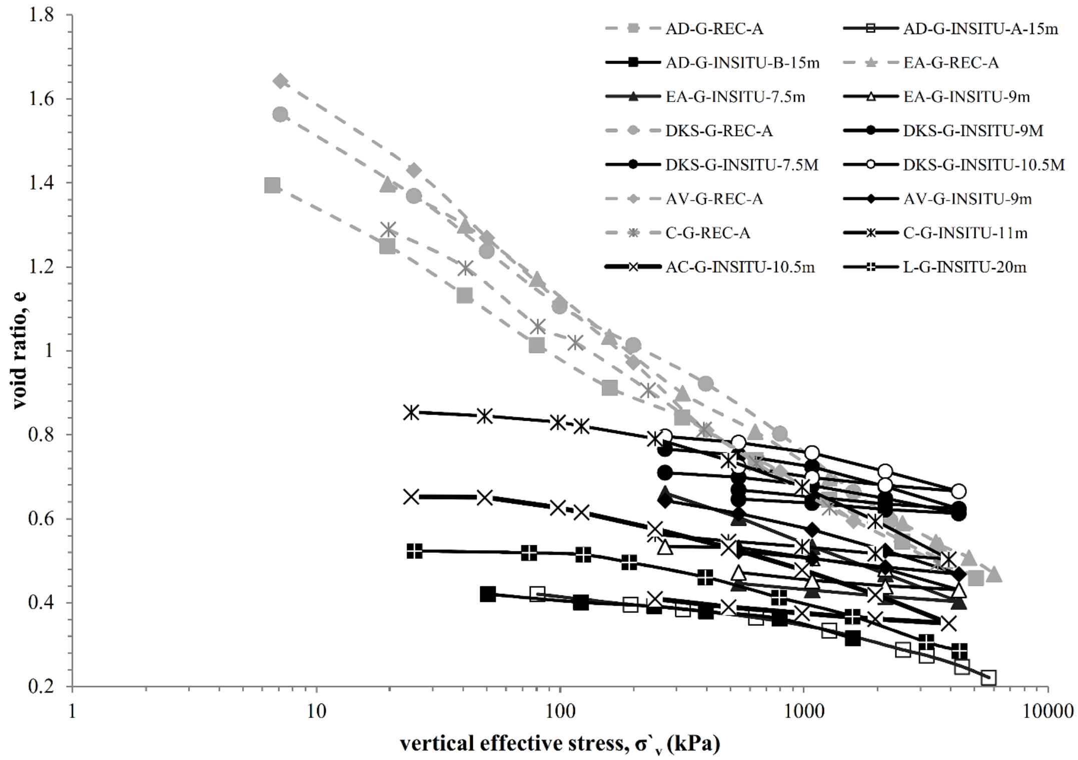

Fig. 6. One dimensional compression of reconstituted and cemented marine deposited Cyprus clay.

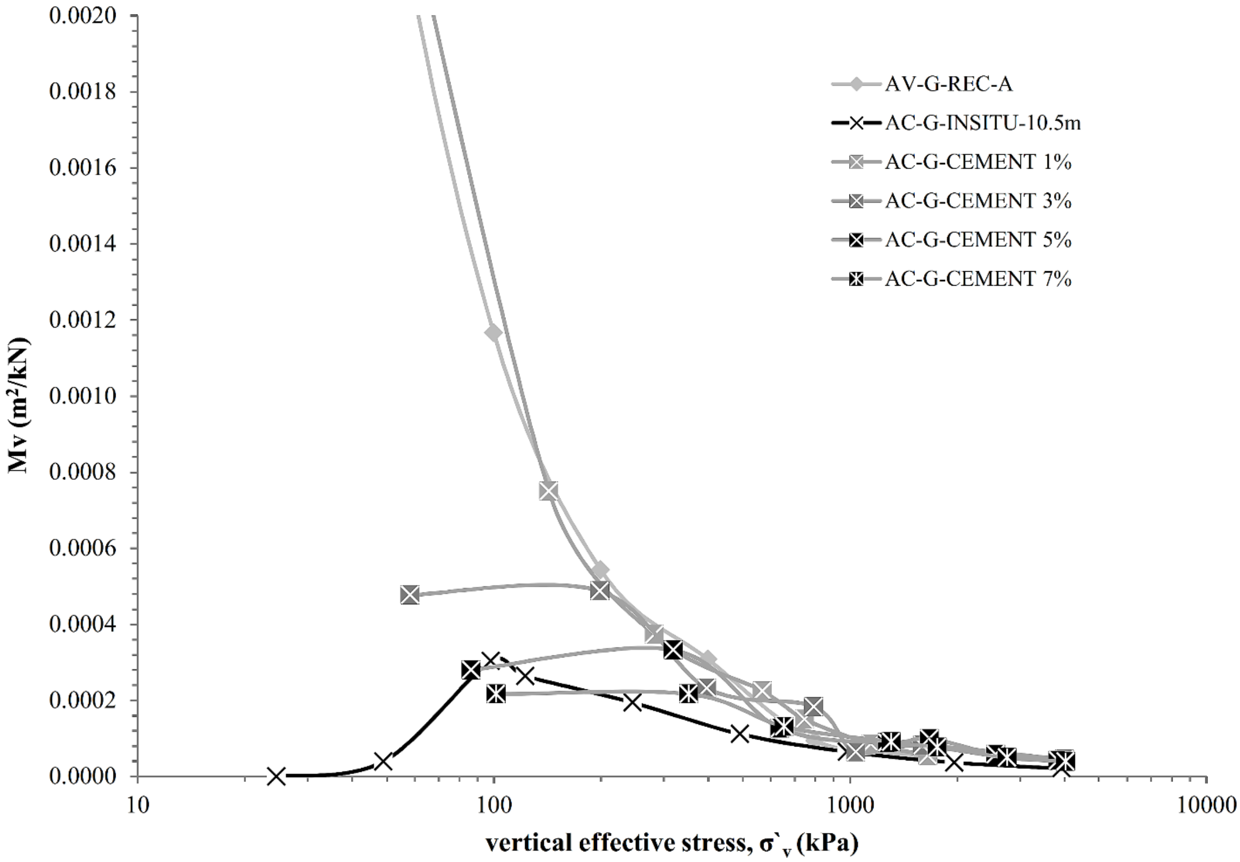

Fig. 7. Coefficient of volume compressibility of in-situ, reconstituted, and cemented specimens.

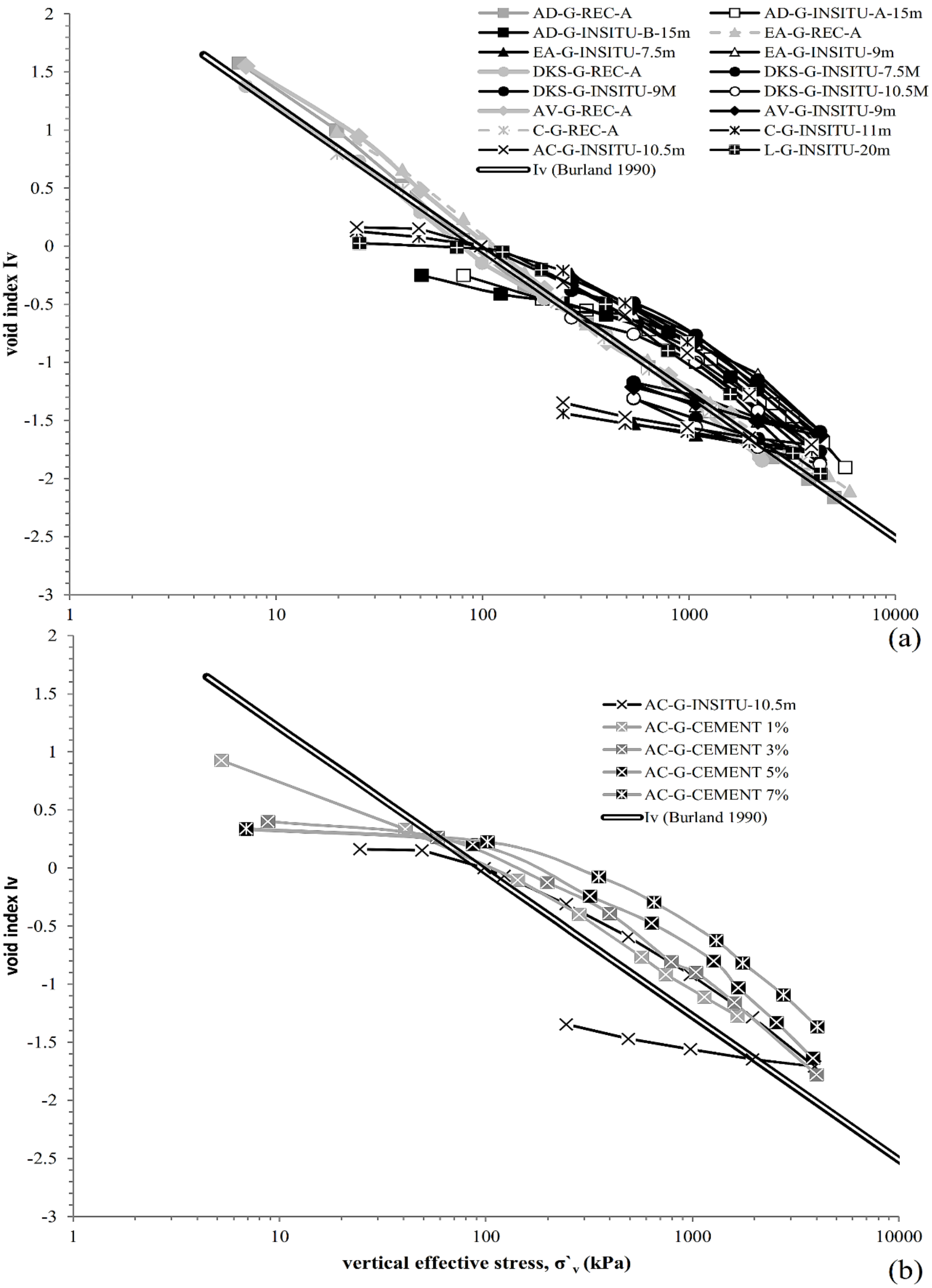

Fig. 8. Results of oedometer tests on (a) undisturbed, reconstituted, and (b) cemented Değirmenlik/Kythrea clays in terms of void index.

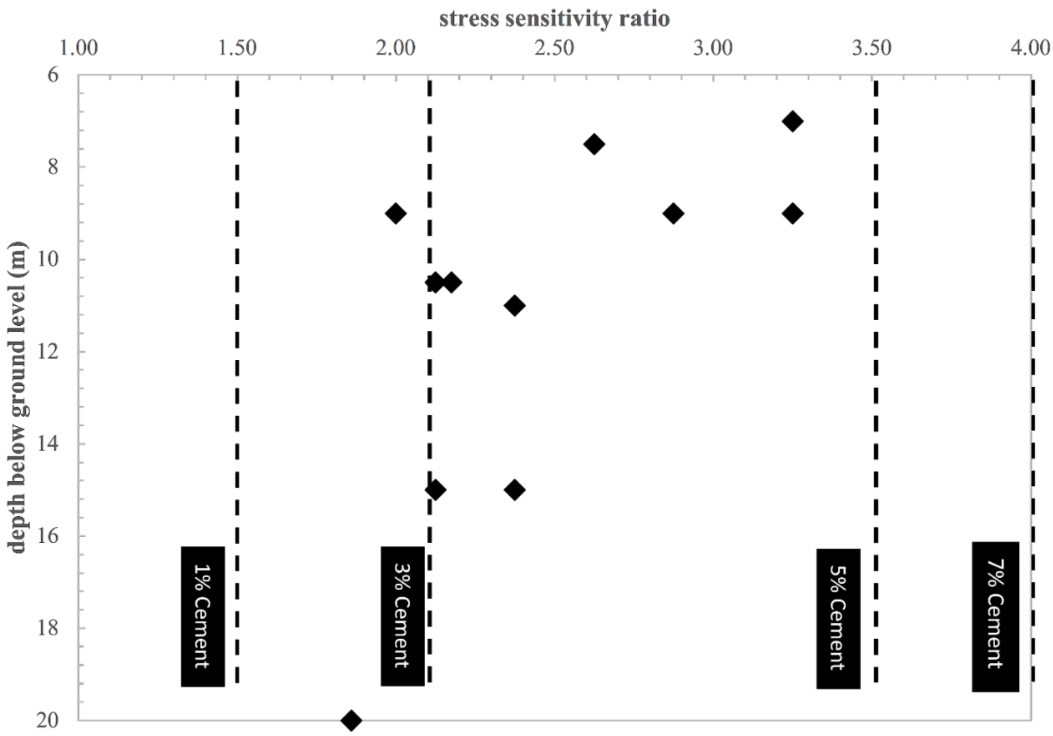

Fig. 9. Stress sensitivity variation with depth and cement content.

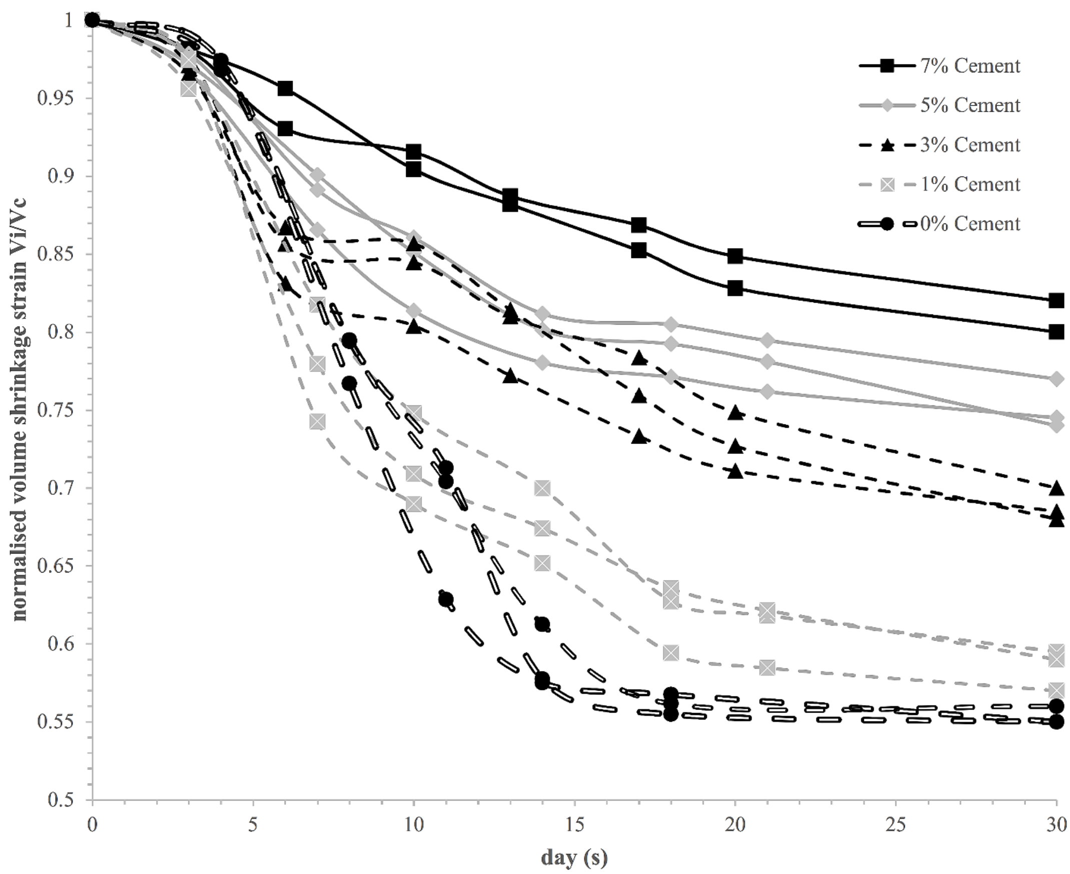

Fig. 10. Change in normalized volume of untreated and cement treated samples caused by drying.

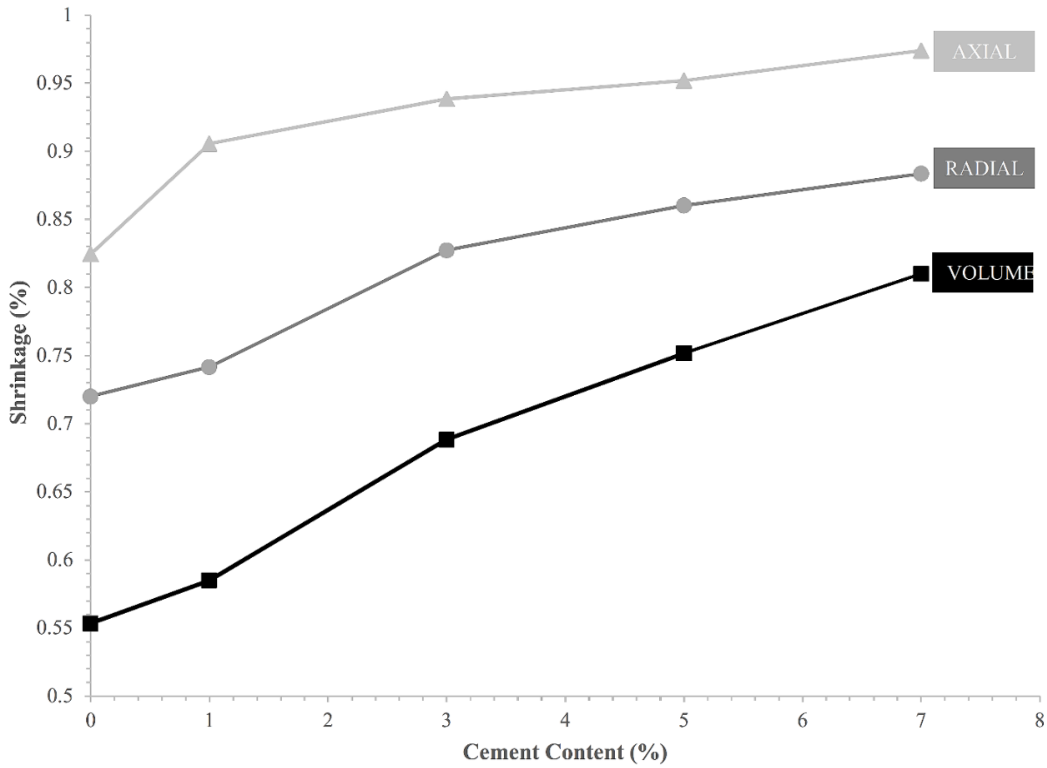

Fig. 11. End of drying period average axial, radial and volume shrinkage of samples.

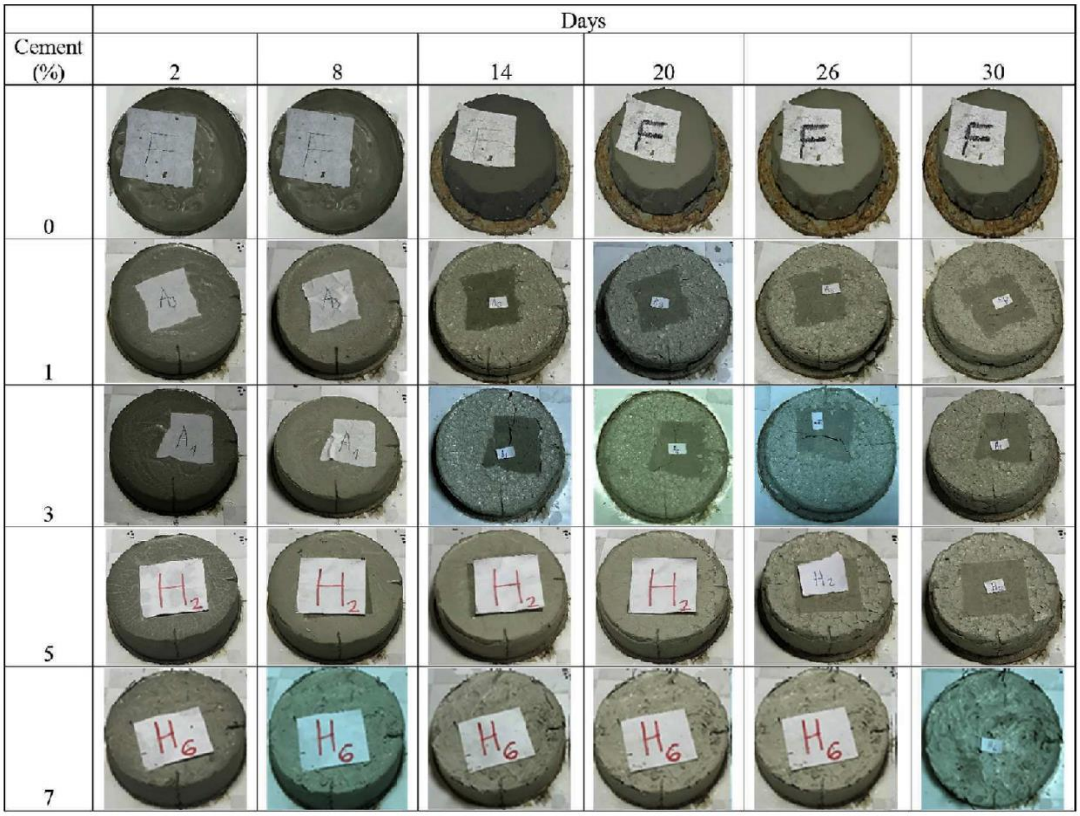

Fig. 12. Photographs of untreated and treated specimens at different intervals of time.

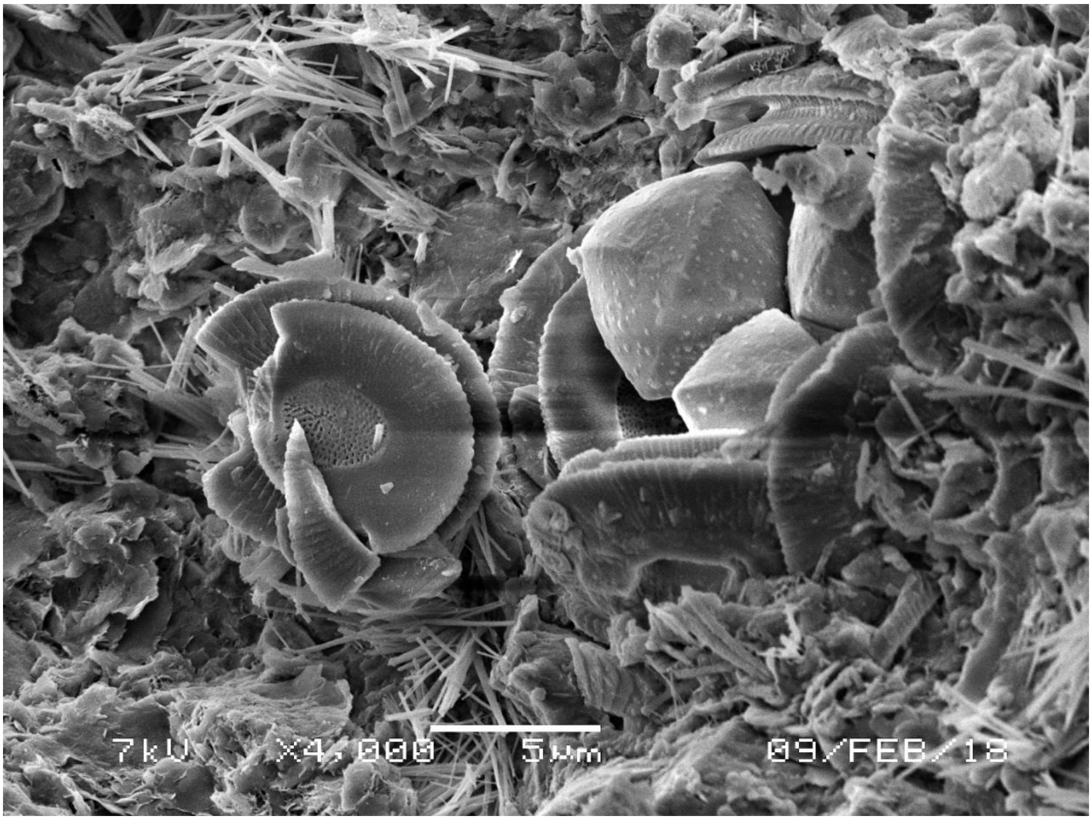

Fig. 13. SEM of Değirmenlik/Kythrea clay treated with 5% Portland cement.

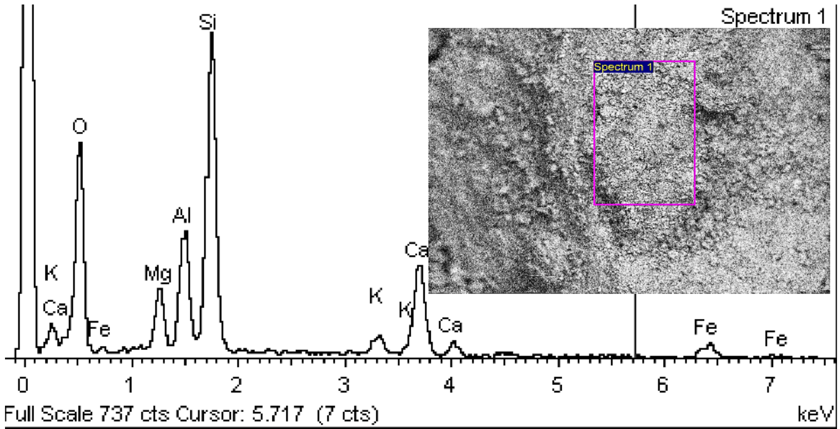

Element	Weight%	Atomic%	Compd%	Formula
Mg K	4.00	3.67	6.64	MgO
Al K	7.95	6.57	15.02	Al2O3
Si K	22.83	18.14	48.85	SiO2
K K	2.32	1.32	2.80	K2O
Ca K	13.33	7.42	18.65	CaO
Fe K	6.27	2.50	8.06	FeO
O	43.30	60.38		
Totals	100.00			

Fig. 14. EDX inspection field: Resulting spectrum and tabulated results of clay treated with 5% Portland cement.

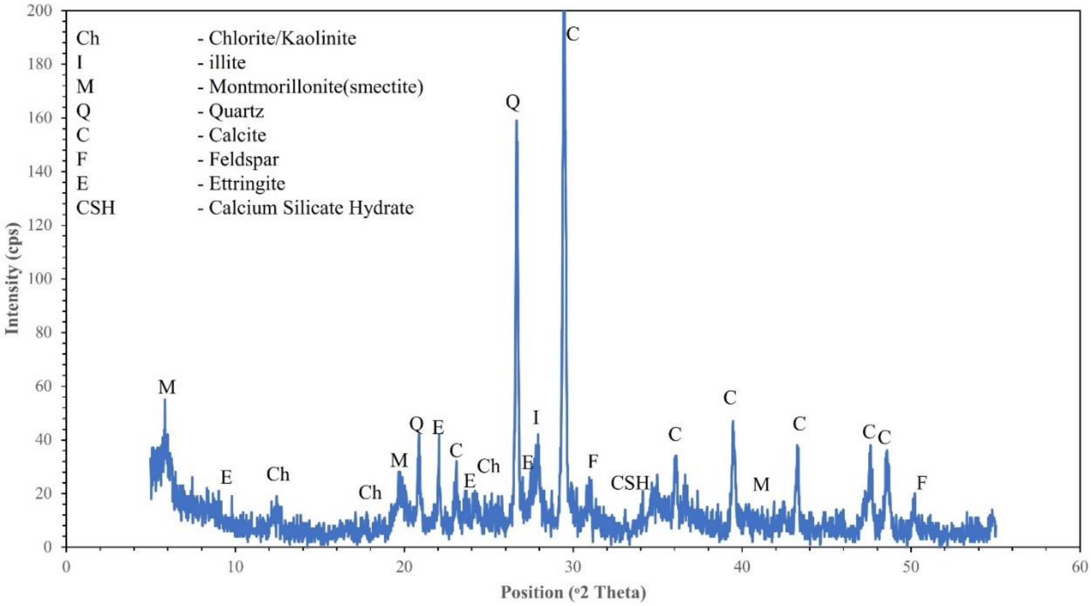

Fig. 15. X-ray diffraction of studied clay-5% cement specimen.

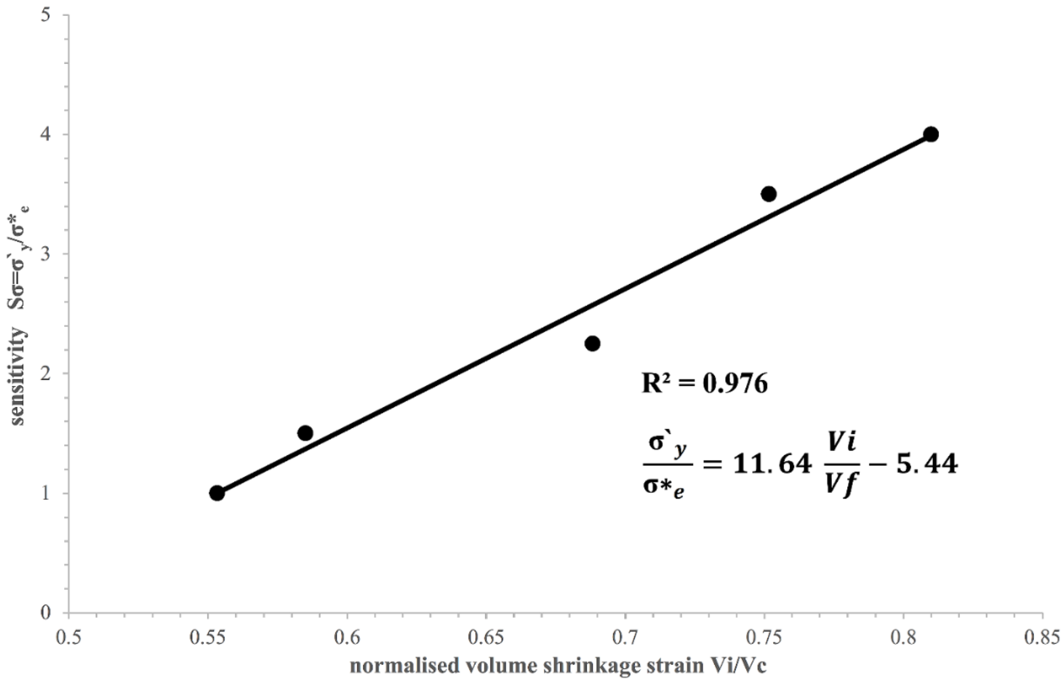

Fig. 16. Relationship between sensitivity ratio and normalized volume shrinkage.